Research Square

Preprints are preliminary reports that have not undergone peer review.
They should not be considered conclusive, used to inform clinical practice,
or referenced by the media as validated information.

# Influence of the response modification factor on the bidirectional seismic performance of reinforced-concrete buildings

**Marco F. Garcia**

mgarciach@continental.edu.pe

Continental University

**Renzo J. Mejia**

Pontifical Catholic University of Peru

**Victor I. Fernandez-Davila**

Pontifical Catholic University of Peru

**Research Article**

**Keywords:** Response modification factor, Bidirectional seismic interaction, Incremental Dynamic Analysis, FEMA P695, Reinforced-concrete buildings, 2DOF systems.

**Posted Date:** August 14th, 2026

**DOI:** https://doi.org/10.21203/rs.3.rs-10506680/v1

**License:** This work is licensed under a Creative Commons Attribution 4.0 International License.
Read Full License

**Additional Declarations:** No competing interests reported.

# Influence of the response modification factor on the bidirectional seismic performance of reinforced-concrete buildings

Marco F. Garcia [a,*], Renzo J. Mejia [b], Victor I. Fernandez-Davila [b]

[a] Section of Civil Engineering, Continental University, Junin, Peru.

[b] Section of Civil Engineering, Pontifical Catholic University of Peru, Lima, Peru.

## ABSTRACT

Although the response modification factor (R) has been extensively studied, most prior work relied on simplified unidirectional systems, limiting applicability to real reinforced-concrete (RC) buildings subjected to bidirectional seismic excitation. This study examines how R influences the seismic performance and collapse capacity of RC buildings using the FEMA P695 methodology and Incremental Dynamic Analysis. Three-dimensional (3D) models of 1-, 2-, 4-, and 8-story RC buildings were analyzed under unidirectional and bidirectional ground motions using nonlinear time-history response analyses (NLTHA) to obtain equivalent systems. In parallel, equivalent two-degree-of-freedom (2DOF) systems with an elliptical bidirectional yield surface and IMK-based hysteretic deterioration were developed as efficient alternatives for collapse assessment. Results show that bidirectional excitation reduced the Collapse Margin Ratio (CMR) by 6.6%–30.1% relative to unidirectional analyses, and compliance with FEMA P695 acceptance criteria required lowering R from 8 to 4–5, depending on the structural system. The proposed 2DOF framework reproduced the 3D median collapse capacity with errors generally below 6%, offering an efficient tool for bidirectional collapse assessment and R calibration.

## Keywords

Response modification factor; Bidirectional seismic interaction; Incremental Dynamic Analysis; FEMA P695; Reinforced-concrete buildings; 2DOF systems.



* Corresponding author. Section of Civil Engineering, Continental University, 1980 San Carlos Avenue, Huancayo 12001, Peru.
E-mail addresses: mgarciach@continental.edu.pe (M. Garcia), renzo.mejiat@pucp.pe (R. Mejia), vfernandezdavila@pucp.edu.pe (V. Fernandez-Davila)

## 1. Introduction

Modern seismic design allows controlled inelastic excursions during severe earthquakes, thereby reducing elastic forces through response modification factors R; otherwise, structures would become excessively robust and expensive. The concept of reducing elastic forces based on the inelastic capacity of structural systems originates from classical studies of the inelastic behavior of simple systems subjected to seismic excitation (Veletsos and Newmark, 1960; Clough, 1966). Although the widespread use of these factors R was initially influenced by engineering judgment and observations of the performance of different structural systems during past earthquakes (Miranda and Bertero, 1994), numerous studies later proposed rational formulations to estimate strength reduction factors as a function of parameters such as the natural vibration period, target displacement ductility, damping ratio, site conditions, and characteristics of ground motions (Riddell and Newmark, 1979; Riddell et al., 1989; Nassar and Krawinkler, 1991; Miranda, 1993; Miranda and Bertero, 1994; Genshu and YongFeng, 2007; Bazan and Fernandez-Davila, 2020; Garcia et al., 2023, Garcia et al., 2024). These studies demonstrated that the reduction factor is not constant and depends strongly on both structural and seismic parameters, particularly for short- and intermediate-period systems. However, many of these evaluations were performed using unidirectional single-degree-of-freedom (SDOF) systems (except for the latter-cited study), which limit their direct applicability to real multiple-degrees-of-freedom (MDOF) buildings subjected to bidirectional seismic excitation.

Furthermore, as the Performance-Based Earthquake Engineering (PBEE) framework and advanced nonlinear analysis procedures were developed, there emerged a need to explicitly relate design parameters to structural performance metrics and collapse probability (NIST, 2010). The Incremental Dynamic Analysis (IDA) methodology has become established as a means of evaluating structural response from the elastic range to global dynamic instability by progressively scaling real earthquake ground motions (Vamvatsikos and Cornell, 2002a). The subsequent systematization and practical implementation of IDA demonstrated its ability to identify structural collapse, quantify record-to-record variability, and relate seismic intensity measures (IM) to structural limit states (Vamvatsikos, 2004; Vamvatsikos, 2007).

In this context, the FEMA P695 methodology was developed to evaluate and calibrate seismic performance factors (including the response modification factor R) using nonlinear collapse simulations within a probabilistic framework (FEMA, 2009; NIST, 2010). This procedure verifies whether a structural system designed with a given R meets acceptable collapse-probability levels while accounting for uncertainties in seismic demand and structural capacity. Subsequent studies applied this methodology to various structural systems, demonstrating that collapse probability depends strongly on parameters such as structural configuration, ductility capacity, collapse mechanisms, and modeling uncertainties (Haselton et al., 2011; Liel et al., 2011). These findings underscore that the selection of the factor R must be properly linked to the actual nonlinear behavior of the structural system.

Despite methodological advances in recent decades, many studies evaluating strength reduction factors still rely on unidirectional (UNI) analyses. In real structural systems, earthquake excitation occurs simultaneously in multiple horizontal directions, and the structural response may be significantly influenced by interactions among resisting

components. Several investigations have shown that both the orientation of ground motions and bidirectional (BID) interaction can substantially modify inelastic demands and nonlinear response patterns (Stewart et al., 2011; Reyes and Kalkan, 2015a; Reyes and Kalkan, 2015b; Aparna et al., 2018; Kwong and Chopra, 2018). In addition, it has been demonstrated that the angle of incidence and the combination of horizontal seismic components may lead to higher structural demands than UNI analyses, particularly within the post-elastic range (Fernandez-Davila et al., 2000; Fernandez-Davila and Cruz, 2008; Hussain et al., 2022a; Wang et al., 2023). Experimental and numerical studies on RC columns and frame systems subjected to biaxial excitation have further shown that inelastic interaction can reduce the effective plastic rotation capacity and modify the mechanisms of stiffness degradation (Ozcan and Binici, 2022). Similarly, analyses of buildings designed in accordance with modern seismic codes indicate that BID excitation may significantly reduce CMRs compared with conventional unidirectional assessments (Gwalani et al., 2022).

In parallel, simplified models have been proposed to capture bidirectional interactions using elliptical yield surfaces and coupled hysteretic formulations (De Stefano y Faella, 1996; Hussain et al., 2022a; Hussain et al., 2022b), enabling the evaluation of coupled bidirectional behavior in single-mass, two-degree-of-freedom (2DOF) discrete systems. Wang et al. (2023) and Garcia et al. (2024) suggest that BID interaction may increase lateral strength demands and modify the effective value of the response modification factor when both horizontal components are considered simultaneously. Despite these advances, a significant gap remains between the parametric evaluation of simplified systems (SDOF/2DOF) and the verification of real buildings designed according to current seismic code provisions, particularly when combining: (i) variable response modification factors, (ii) consistent bidirectional seismic assessment, and (iii) probabilistic validation through the FEMA P695 methodology. In particular, the quantification of the error associated with using simplified bidirectional models as preliminary substitutes for complete three-dimensional structural models has not been systematically investigated within a collapse assessment framework.

Given the above, this study investigates how the response modification factor R affects the bidirectional seismic performance of RC buildings. The collapse capacity of 3D building models is compared with that of equivalent 2DOF systems that use an elliptical yield surface to capture bidirectional interaction. The evaluation is conducted using IDA and collapse assessment procedures in accordance with FEMA P695 (FEMA, 2009). The objectives are to: (i) quantify the influence of the response modification factor R on structural performance under UNI and BID seismic excitation, and (ii) evaluate the ability of equivalent 2DOF systems to provide reliable collapse predictions while offering a computationally efficient alternative to 3D building models. This paper may contribute to improving engineering practice and future seismic design methodologies by providing a computationally efficient approach for bidirectional collapse assessment and response modification factor calibration.

## 2. Earthquake ground motions

A total of 30 pairs of seismic acceleration records (horizontal components only) were used in this study. The records were selected from the NGA Subduction Portal of the National Hazards Risk and Resiliency Research Center (NHR3)

at the University of California, Los Angeles (Mazzoni, 2022) for seismic events in Peru and Chile. According to the Peruvian regulation (MVCS, 2026) (E.030 or NTE.030 for its acronym in Spanish), the selected earthquake ground motions were classified as soil type $S_1$ - hard soil (compatible with site class C: very dense soil and soft rock (ASCE, 2017)). In addition, the seismic records have Peak Ground Acceleration (PGA) values greater than 0.19 g, and Peak Ground Velocity (PGV) values greater than 10 cm/sec. Table 1 summarizes the key characteristics of the seismic acceleration records used in this study.

**Table 1**
Seismic acceleration records.

| Id | Seismic event location | Epicentral Coordinates | | Year | Magnitude [Mw] | Epicentral Distance [km] | PGA [g] | PGV [cm/s] |
|---|---|---|---|---|---|---|---|---|
| | | [Lat.] | [Long.] | | | | | |
| 1 | Arequipa, Peru | -16.21 | -73.62 | 2001 | 8.41 | 306.77 | 0.30 | 29.86 |
| 2 | Arequipa, Peru | -16.21 | -73.62 | 2001 | 8.41 | 452.40 | 0.26 | 29.94 |
| 3 | Antofagasta, Chile | -22.34 | -70.02 | 2007 | 7.75 | 102.09 | 0.32 | 10.99 |
| 4 | Antofagasta, Chile | -22.34 | -70.02 | 2007 | 7.75 | 95.06 | 0.42 | 36.28 |
| 5 | Antofagasta, Chile | -22.34 | -70.02 | 2007 | 7.75 | 33.18 | 0.69 | 23.92 |
| 6 | Antofagasta, Chile | -22.34 | -70.02 | 2007 | 7.75 | 33.55 | 0.41 | 18.09 |
| 7 | Near Arica / Oruro, Chile-Peru border | -19.64 | -70.82 | 2014 | 8.15 | 120.17 | 0.26 | 19.46 |
| 8 | Near Arica / Oruro, Chile-Peru border | -19.64 | -70.82 | 2014 | 8.15 | 122.31 | 0.73 | 29.10 |
| 9 | Arequipa, Peru | -16.21 | -73.62 | 2001 | 8.41 | 452.40 | 0.25 | 29.18 |
| 10 | Melipilla / San Antonio, Chile | -33.13 | -71.61 | 1985 | 7.98 | 92.59 | 0.42 | 17.70 |
| 11 | Melipilla / San Antonio, Chile | -33.13 | -71.61 | 1985 | 7.98 | 172.04 | 0.34 | 24.49 |
| 12 | Concepcion, Biobio, Chile | -36.21 | -72.96 | 2010 | 8.81 | 315.20 | 0.34 | 44.19 |
| 13 | Concepcion, Biobio, Chile | -36.21 | -72.96 | 2010 | 8.81 | 362.11 | 0.27 | 27.27 |
| 14 | Concepcion, Biobio, Chile | -36.21 | -72.96 | 2010 | 8.81 | 322.34 | 0.77 | 49.66 |
| 15 | Concepcion, Biobio, Chile | -36.21 | -72.96 | 2010 | 8.81 | 368.64 | 0.24 | 22.03 |
| 16 | Concepcion, Biobio, Chile | -36.21 | -72.96 | 2010 | 8.81 | 206.38 | 0.47 | 37.28 |
| 17 | Concepcion, Biobio, Chile | -36.21 | -72.96 | 2010 | 8.81 | 364.13 | 0.26 | 32.00 |
| 18 | Concepcion, Biobio, Chile | -36.21 | -72.96 | 2010 | 8.81 | 374.36 | 0.31 | 16.68 |
| 19 | Near Arica/Oruro, Chile-Peru border | -19.64 | -70.82 | 2014 | 8.15 | 102.91 | 0.45 | 35.12 |
| 20 | Iquique, Tarapaca, Chile | -20.52 | -70.47 | 2014 | 7.76 | 47.61 | 0.19 | 11.41 |
| 21 | Iquique, Tarapaca, Chile | -20.52 | -70.47 | 2014 | 7.76 | 48.17 | 0.21 | 10.45 |
| 22 | La Serena / Coquimbo, Chile | -31.56 | -71.66 | 2015 | 8.31 | 122.21 | 0.69 | 30.81 |
| 23 | La Serena / Coquimbo, Chile | -31.56 | -71.66 | 2015 | 8.31 | 174.57 | 0.34 | 38.18 |
| 24 | Iquique, Tarapaca, Chile | -20.52 | -70.47 | 2014 | 7.76 | 47.72 | 0.45 | 15.73 |
| 25 | La Serena / Coquimbo, Chile | -31.56 | -71.66 | 2015 | 8.31 | 116.77 | 0.83 | 38.84 |
| 26 | La Serena / Coquimbo, Chile | -31.56 | -71.66 | 2015 | 8.31 | 98.23 | 0.35 | 21.23 |
| 27 | Vicuna, Coquimbo, Chile | -30.79 | -71.42 | 2015 | 6.3 | 91.86 | 0.64 | 26.14 |
| 28 | Near Arica/Oruro, Chile-Peru border | -19.64 | -70.82 | 2014 | 8.15 | 95.47 | 0.29 | 18.17 |
| 29 | Near Arica/Oruro, Chile-Peru border | -19.64 | -70.82 | 2014 | 8.15 | 154.01 | 0.28 | 25.02 |
| 30 | Iquique, Tarapaca, Chile | -20.52 | -70.47 | 2014 | 7.76 | 46.30 | 0.53 | 18.79 |

The seismic records were processed in accordance with FEMA P695 regulations (FEMA, 2009). First, the horizontal component with the highest Specific Density Energy (SED) was aligned with the X-axis ($\ddot{u}_{gx}$). This intensity measure, developed by Sarma and Yang in 1987 (Sarma and Yang, 1987), represents the total energy of the earthquake as the integral of the square of the velocity (Kalman et al., 2025). Then, the pair of seismic acceleration records was normalized by a scale factor using Eqs. (1) and (2).

$$N_{f,i} = \frac{Median(\overline{PGV_i})}{\overline{PGV_i}} \quad (1)$$

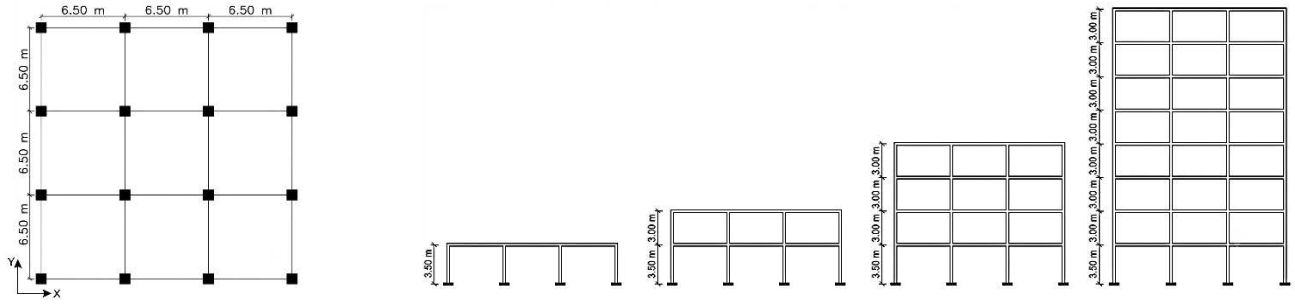
$$\ddot{U}_{gx,i} = N_{f,i} \cdot \ddot{u}_{gx,i} \quad , \quad \ddot{U}_{gy,i} = N_{f,i} \cdot \ddot{u}_{gy,i} \quad (2)$$

Where: $N_{f,i}$ is the normalization factor of both horizontal components of the $i^{th}$ record; $\overline{PGV_i}$ represents the geometric mean of the peak ground velocities along the $x$ and $y$ components ($PGV_{x,i}$ and $PGV_{y,i}$, respectively); $\ddot{u}_{gx,i}$ (or $\ddot{u}_{gy,i}$) is the seismic acceleration record $i$ along the $x$ (or $y$) component; and $\ddot{U}_{gx,i}$ (or $\ddot{U}_{gy,i}$) is the normalized seismic acceleration record $i$ along the $x$ (or $y$) component. It is worth noting that the SED ratio between the secondary ($y$ component) and principal ($x$ component) directions was at least 25%. This scaling process is a simple way to reduce unwarranted variability between records arising from inherent differences in their characteristics (event magnitude, distance to the source, source type, site conditions). Nevertheless, inherent aleatory variability (i.e., record-to-record variability) is preserved. Structural systems with bidirectional interaction are sensitive to the $N_f$ used, because of the coupling effect between the two components' responses (Garcia et al., 2024). Although the structural responses were computed for both horizontal components, only those in the global X-axis are presented in the present study, as the principal horizontal component of each ground-motion record was assigned to this direction.

## 3. Modeling of the building structures

### *3.1. General characteristics of the buildings*

Four three-dimensional RC buildings (1-, 2-, 4-, and 8-story structures, each with the same plan configuration) were designed and analyzed to investigate the effects of unidirectional and bidirectional seismic excitations on their seismic performance. The buildings are denoted as 1S, 2S, 4S, and 8S, respectively. The typical floor plan of the buildings considered is shown in Fig. 1(a), while the elevations and story heights are shown in Fig. 1(b). The first-story height is 3.5 m, whereas the height of all upper stories is 3.0 m. The span length is 6.50 m in both principal directions.




(a) (b)

**Figure 1.** (a) Plan of the considered buildings (symmetric RC frame buildings); (b) Height of RC frame buildings.

All the buildings were designed for combined gravity and seismic loads as "RC frame buildings" in accordance with Peruvian regulations (MVCS, 2026; MVCS, 2009). In this study, the buildings are located in the region of highest seismic hazard in Peru, specifically Seismic Zone 4 (Z = 0.45) (MVCS, 2026). This corresponds to a maximum acceleration of 0.45·g for the Design Earthquake with a 10% probability of exceedance in 50 years (equivalent to a 475-year return

period). Nevertheless, the evaluation of seismic performance in accordance with FEMA P695 (FEMA, 2009) must be based on seismic hazard values with a 2% probability of exceedance in 50 years (equivalent to a 2475-year return period). This is usually referred to as the Maximum Considered Earthquake (MCE) and can reach up to 150% of the Design Earthquake's intensity.

### *3.2. Linear analysis and design*

Peruvian regulations (MVCS, 2026; MVCS, 2009) were used for the linear analysis and design of the buildings. Three-dimensional models were developed using frame elements for columns and beams, and membrane elements for slabs. The slabs acted as rigid diaphragms in their own plane, transferring gravity loads to the supporting beams. The fundamental vibration periods were estimated using the code-prescribed empirical height-based expression. The buildings were then designed using the modal response spectrum analysis method. In accordance with (MVCS, 2026), the code-prescribed 100–30 orthogonal seismic loading criterion was adopted, in which 100% of the seismic action in one principal direction is combined with 30% of the action in the orthogonal direction. Accidental torsional effects were considered by applying a 5% eccentricity of the center of mass relative to the building dimension perpendicular to the loading direction. The design base shear was determined from the fundamental vibration period and adjusted as needed to meet minimum code requirements. The properties of the analyzed buildings are presented in Table 2. Because of the symmetric plan configuration, the fundamental vibration periods are identical in both principal directions ($T_x = T_y$).

The sizes of the structural members were proportioned to achieve longitudinal reinforcement ratios of 1.0%–3.0% in columns and 0.24%–1.6% in beams, consistent with (MVCS, 2009). However, for beams in buildings designed with low response modification factors, the reinforcement restrictions applicable to doubly reinforced sections were enforced. The structural members have ductile reinforcement detailing and capacity design to avoid brittle shear failure, as established in relevant codes. All beams and columns conform to the Strong Column–Weak Beam (SC–WB) design criterion, maintaining a minimum moment capacity ratio of 1.20 (MVCS, 2009).

**Table 2**
Properties of the analyzed buildings.

| **Building model** | | **Fundamental vibration period [sec]** | **Design base shear coefficient [$C_s$]** | **Rectangular cross-sectional properties [mm x mm]** | |
|---|---|---|---|---|---|
| **ID** | **Story** | $T_x = T_y$ | | **Beams** | **Columns** |
| 1S | 1-story | 0.10 | 0.141 | 250 x 450 | 450 x 450 |
| 2S | 2-story | 0.19 | 0.141 | 250 x 500 | 500 x 500 |
| 4S | 4-story | 0.36 | 0.141 | 300 x 600 (1° to 2°)*<br>250 x 500 (3° to 4°) | 650 x 650 |
| 8S | 8-story | 0.70 | 0.080 | 300 x 600 (1° to 6°)<br>250 x 500 (7° to 8°) | 800 x 800 (1° to 2°)<br>700 x 700 (3° to 5°)<br>600 x 600 (6° to 8°) |

(*) Floor levels.

### *3.3. Nonlinear modeling*

The nonlinear modeling of the 3D building was performed using OpenSees v.3.8.0 (McKenna, 1997). Nonlinear behavior was modeled by assuming concentrated plasticity in the beams and distributed plasticity in the columns. These properties are discussed below. The nonlinear analyses were performed using the expected material strengths recommended by the Chilean guidelines (Achisina, 2017). Accordingly, the expected compressive strength of concrete and the expected yield strength of the reinforcing steel bars were taken as $1.3 \cdot f_c'$ and $1.17 \cdot f_y$, respectively, resulting in values of 26.8 MPa for concrete and 481.9 MPa for reinforcing steel. The corresponding design strengths are $f_c' = 20.6\,MPa$ and $f_y = 411.9\,MPa$, which are commonly adopted in Peruvian RC design.

For the beams, a lumped plasticity hinge model was used to represent inelastic behavior. Uniaxial moment–rotation plastic hinges were assigned at both beam ends and connected via elastic beam-column elements using the *ConcentratedPlasticity* beam integration scheme (Mazzoni and Scott, 2024). The backbone curves (i.e., the moment-rotation envelope) were defined according to the criteria proposed by Haselton et al. (2016). These criteria are similar to those in the ASCE 41-23 provisions (ASCE, 2023), but they exhibit gradual post-capping strength degradation rather than a sudden drop. Such a sudden drop in strength is somewhat unrealistic and can lead to instability in the numerical solution (Gwalani et al., 2021). The Ibarra-Medina-Krawinkler (IMK) model (Ibarra et al., 2005) was employed to capture the nonlinear structural response over time. This model considers four deterioration modes: basic strength deterioration, post-capping strength deterioration, unloading stiffness deterioration, and accelerated reloading stiffness deterioration.

For the columns, the *forceBeamColumn* element was used to capture the distributed inelastic response along the member length. This force-based formulation discretizes the element into several integration points, where the sectional response is evaluated, and employs the Gauss–Lobatto quadrature rule to compute the element stiffness matrix efficiently (Taucer et al., 1991; Durufle et al., 2009). In this study, five integration points were adopted. Material nonlinearity was represented using the fiber-section approach, in which the cross-section is discretized into steel and concrete fibers, each governed by uniaxial stress–strain relationships, and the sectional response is obtained by integrating the responses of all fibers (Kashani et al., 2017). The reinforcing steel's stress-strain behavior was described by the nonlinear Menegotto and Pinto (1973) model, as modified by Fillipou et al. (1983) to include isotropic strain hardening (implemented in the *Steel02* material in OpenSees). The model is computationally efficient and agrees very well with experimental results from cyclic tests on reinforcing steel bars (Taucer et al., 1991). The monotonic envelope curve for concrete compression follows the Kent and Park (1973) model, later extended by Scott et al. (1982) (implemented in the *Concrete02* material in OpenSees). Although more accurate and complete models have since been published, the so-called modified Kent and Park model offers a good balance between simplicity and accuracy (Taucer et al., 1991).

The structural model represents beam–column joints implicitly through rigid end offsets, without explicitly modeling the panel zone. This approach simplifies the computational framework while preserving essential kinematic compatibility and force transfer at beam–column interfaces. This modeling approach is conceptually consistent with the rigid beam–column joint assumption commonly used in nonlinear frame analysis, in which joint deformation is neglected, and inelasticity is concentrated in adjacent frame elements. Bond-slip effects at the base of the columns were explicitly modeled using *zeroLengthSection* elements, thereby accounting for reinforcement slip at the column–foundation interface. The modeling strategy is sufficiently comprehensive to reliably simulate the dynamic response of buildings subjected to unidirectional and bidirectional ground motions, as schematically illustrated in Fig. 2.

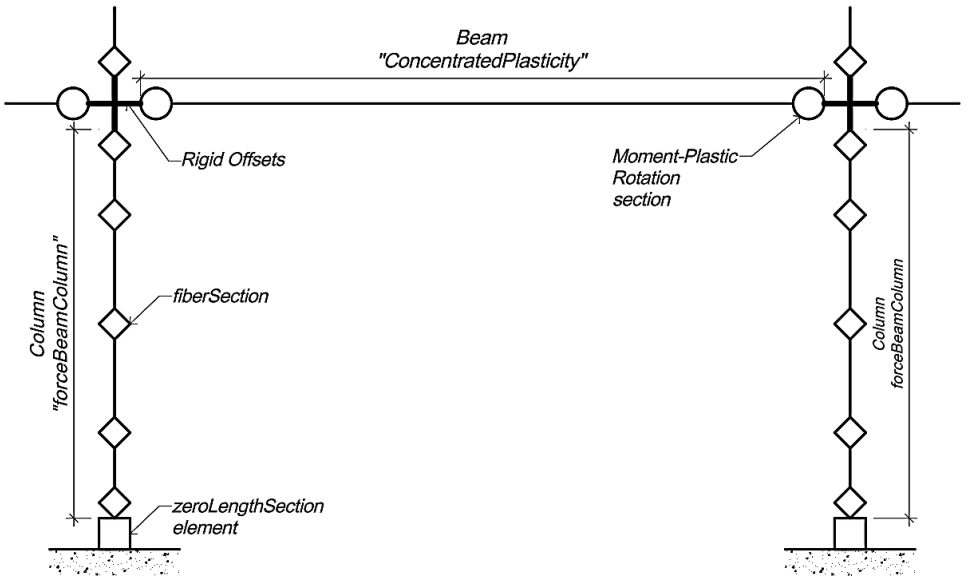



**Figure 2.** Schematic of the nonlinear modeling strategy used.

### *3.4. Nonlinear analysis*

Incremental Dynamic Analysis (IDA) is an advanced seismic assessment method in which a nonlinear structural model is subjected to a suite of real ground-motion records, each incrementally scaled to explore structural behavior from the elastic range to global dynamic instability or collapse. This technique produces IDA curves that relate Seismic Intensity Measures (IM) to Engineering Demand Parameters (EDP), providing a comprehensive view of seismic demand and structural capacity across varying levels of ground-motion severity. IDA has proven particularly powerful within the framework of PBEE, enabling precise quantification of limit states, evaluation of uncertainties, and estimation of mean annual exceedance frequencies for significant damage or collapse (Vamvatsikos and Cornell, 2002a; Vamvatsikos and Cornell, 2002b).

Dynamic instability, or collapse, is considered to occur when a slight increase in the IM produces an abrupt increase in the EDP (Gwalani et al., 2021). To identify the collapse state, both simulated and non-simulated collapse metrics were used. The simulated collapse criterion was defined as a 10% reduction in lateral stiffness, whereas the non-simulated collapse criteria were based on reinforcing steel compressive and tensile strain limits of 0.025 and 0.05, respectively.

These criteria align with the collapse assessment framework proposed by Gwalani et al. (2021), who calibrated simulated and non-simulated collapse metrics against experimental data for RC columns subjected to bidirectional loading. Because the estimated collapse capacity depends strongly on the selection of an appropriate IM, the 5%-damped spectral acceleration at the structure's fundamental vibration period, $S_a(T_1, 5\%)$, was adopted for its efficiency and widespread use in nonlinear dynamic analyses. For the evaluation under bidirectional ground motions and considering buildings with equal code-defined fundamental vibration periods in the two principal directions ($T_x = T_y$), the geometric mean of the spectral accelerations in the $x$ and $y$ components was used as the effective IM to consistently represent the combined effects of the horizontal seismic excitations.

For each ground-motion record, the same scaling factor was applied to both horizontal components, preserving their original relative amplitudes. For each building model, dynamic capacity curves were developed using IDA, and seismic performance was evaluated in the following sections.

## 4. Modeling of the 2DOF systems

### *4.1. Characterization and analysis of the 2DOF systems*

Two-degree-of-freedom (2DOF) systems follow the fundamental concepts of the Modified Modal Pushover Analysis (MMPA) proposed by Goel and Chopra (2005), which represents the nonlinear response of a multi-degree-of-freedom (MDOF) structure using an equivalent system based on the fundamental mode of vibration. In the present study, a nonlinear static pushover analysis was first conducted using a lateral load pattern proportional to the first-mode shape. The resulting capacity curve $V_{bn} - u_{rn}$ was then idealized (Fig. 3.a) and transformed into the normalized $F_{sn}/L_n - D_n$ format following the MMPA procedure, thereby defining the constitutive relationship of the equivalent 2DOF system (Fig. 3.b).

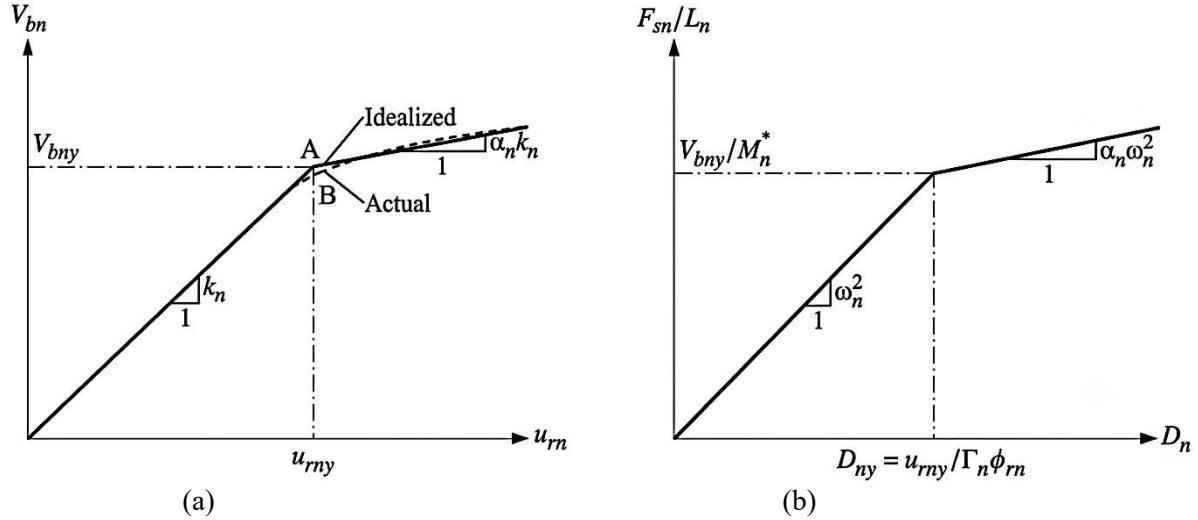



**Fig. 3.** (a) Bilinear idealization of the capacity curve for the fundamental-mode force pattern. (b) Constitutive model of the equivalent 2DOF system associated with the fundamental mode in the analysis direction. (Adapted from Chopra and Goel, 2002)

In Fig. 3.a, corresponding to the MDOF system, $V_{bn}$ is the base shear, $V_{bny}$ is the idealized yield base shear, $k_n$ is the initial elastic stiffness, $u_{rn}$ is the roof displacement, $u_{rny}$ is the roof yield displacement, and $\alpha_n$ is the post-yield stiffness ratio. In Fig. 3.b, corresponding to the equivalent 2DOF system, $F_{sn}/L_n$ is the normalized idealized resistance, $D_n$ is the generalized displacement, $\Gamma_n$ is the modal participation factor, $\phi_{rn}$ is the mode amplitude at the roof level, $D_{ny}$ is the generalized yield displacement, $M_n^*$ is the effective modal mass, and $\omega_n$ is the natural circular frequency. As discussed previously, the subscript $n$ refers to the first vibration mode.

Unlike the conventional MMPA, the proposed approach directly applies UNI and BID ground motions to the equivalent system through NLTHA. The computed responses are then transformed back into the corresponding building responses using the modal transformation relationships, enabling a direct comparison between the equivalent systems and the original three-dimensional building models. The governing equations of motion for the proposed bidirectional 2DOF system are presented in the next section.

*4.2. Equation of motion of 2DOF system*

By solving Eq. (3) for dynamic equilibrium, the seismic response of single-lumped-mass, two-degree-of-freedom (2DOF) systems subjected to bidirectional ground motions can be obtained.

$$\begin{bmatrix} m & 0 \\ 0 & m \end{bmatrix} \cdot \begin{bmatrix} \ddot{u}_x \\ \ddot{u}_y \end{bmatrix} + \begin{bmatrix} 2 \cdot \xi \cdot \sqrt{m \cdot k_x} & 0 \\ 0 & 2 \cdot \xi \cdot \sqrt{m \cdot k_y} \end{bmatrix} \cdot \begin{bmatrix} \dot{u}_x \\ \dot{u}_y \end{bmatrix} + K_T \cdot \begin{bmatrix} u_x \\ u_y \end{bmatrix} = - \begin{bmatrix} m & 0 \\ 0 & m \end{bmatrix} \cdot \begin{bmatrix} \ddot{u}_{gx} \\ \ddot{u}_{gy} \end{bmatrix} \quad (3)$$

Where: $m$ is the single-lumped-mass of the 2DOF system, $\xi$ is the critical damping ratio ($\xi = 3\%$ for this study), $k_x$ (or $k_y$) is the elastic initial stiffness along the $x$ (or $y$) component, $\ddot{u}_x$ (or $\ddot{u}_y$) is the relative acceleration along the $x$ (or $y$) component, $\dot{u}_x$ (or $\dot{u}_y$) is the relative velocity along the $x$ (or $y$) component, $u_x$ (or $u_y$) is the relative lateral displacement along the $x$ (or $y$) component, and $\ddot{u}_{gx}$ (or $\ddot{u}_{gy}$) is the horizontal seismic acceleration record along the $x$ (or $y$) component. To solve Eq. (3), the step-by-step Newmark's method was used, with consideration of the tangent stiffness matrix $K_T$ (Eq. (4)), which depends on the elastic stiffness matrix $K_e$ (Eq. (5)) and the gradient vector $\nabla f$ (Eq. (6)) at each time step. Furthermore, $K_T$ depends on the hysteretic rules of the non-linear behavior model used. The inelastic bidirectional interaction form for the 2DOF systems was determined using a two-dimensional elliptical yield-surface given by Eq. (7).

$$K_T = K_e - [K_e \cdot \nabla f] \cdot [\nabla f^T \cdot K_e \cdot \nabla f]^{-1} \cdot [\nabla f^T \cdot K_e] \quad (4)$$

$$K_e = \begin{bmatrix} k_x & 0 \\ 0 & k_y \end{bmatrix} \quad (5)$$

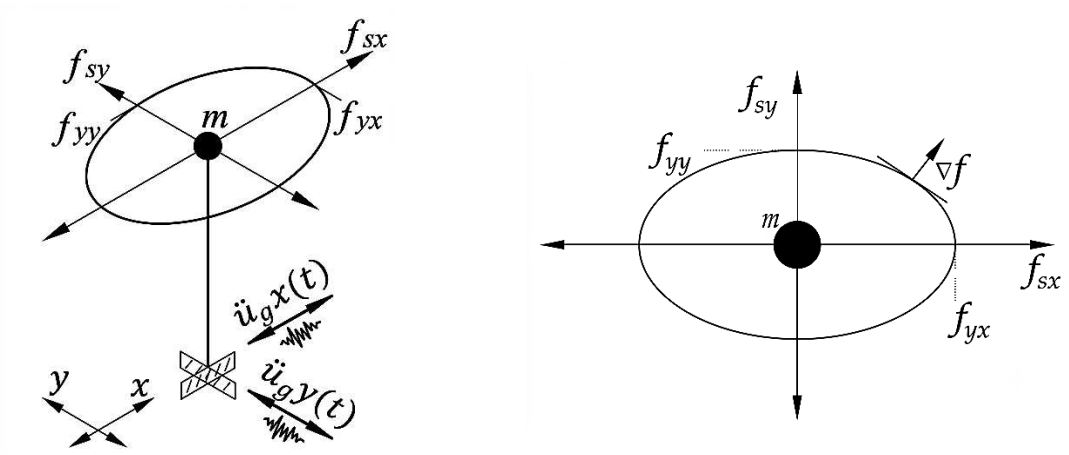
$$\nabla f = \begin{bmatrix} df/df_{sx} \\ df/df_{sy} \end{bmatrix} \quad (6)$$

$$f = \left(\frac{f(x,t)}{f_{yx}}\right)^2 + \left(\frac{f(y,t)}{f_{yy}}\right)^2 \geq 1 \quad (7)$$

Where: $f(x,t)$ (or $f(y,t)$) is the spring hysteretic restoring force along the $x$ (or $y$) component, and $f_{yx}$ (or $f_{yy}$) is the yield force along the $x$ (or $y$) component. Fig. 4 schematizes the two-dimensional elliptical yield surface for a 2DOF system.

*4.3. Hysteretic model with bidirectional interaction*

The nonlinear behavior of the equivalent 2DOF systems was represented using the peak-oriented Ibarra–Medina–Krawinkler (IMK) hysteretic model, originally proposed by Ibarra et al. (2005). A schematic of the adopted IMK model is shown in Fig. 5. Its hysteretic behavior is defined by a trilinear backbone curve characterized by the yield moment ($M_y$), the capping moment ($M_c$), the yield rotation ($\theta_y$), the capping rotation ($\theta_c$), the pre-capping plastic rotation ($\theta_p$), the post-capping plastic rotation ($\theta_{pc}$), and the ultimate rotation ($\theta_u$), together with energy-based cyclic deterioration rules that enable the simulation of cumulative damage effects. The model was selected for its ability to accurately capture the cyclic inelastic response of structural systems, including strength and stiffness deterioration under repeated seismic loading. Owing to its robustness and extensive validation against experimental data, the IMK model has been widely adopted in performance-based seismic assessment, including the FEMA P695 methodology (FEMA, 2009).




(a) (b)

**Figure 4.** (a) Diagram of the 2DOF system subjected to both components of seismic acceleration; (b) Two-dimensional elliptical yield surface. (Adapted from Garcia et al., 2024)

As shown in Fig. 5, the hysteretic rules of the IMK model used are summarized below: Segment 1-2 corresponds to the initial elastic behavior. Segment 2-3 represents the first inelastic incursion, with the post-yield branch defined by $M_y$ and $M_c$. Segment 3-4 describes unloading with stiffness deterioration. Segment 4–5 corresponds to unloading and reloading toward the opposite loading direction, incorporating the stiffness degradation characteristic of the IMK model. Segments 5–6 and 6–7 follow the same hysteretic rules as segments 2–3 and 3–4, respectively. After point 7, the hysteretic cycle is repeated considering the strength and stiffness deterioration mechanisms of the IMK model, represented by the deteriorated backbone curve.

All IDAs for the 2DOF systems were conducted in MATLAB using original scripts developed for this study. The numerical framework includes NLTHA, adaptive ground-motion scaling, collapse-detection criteria, and automated post-processing of EDP. The complete MATLAB scripts used in this study are available upon request.

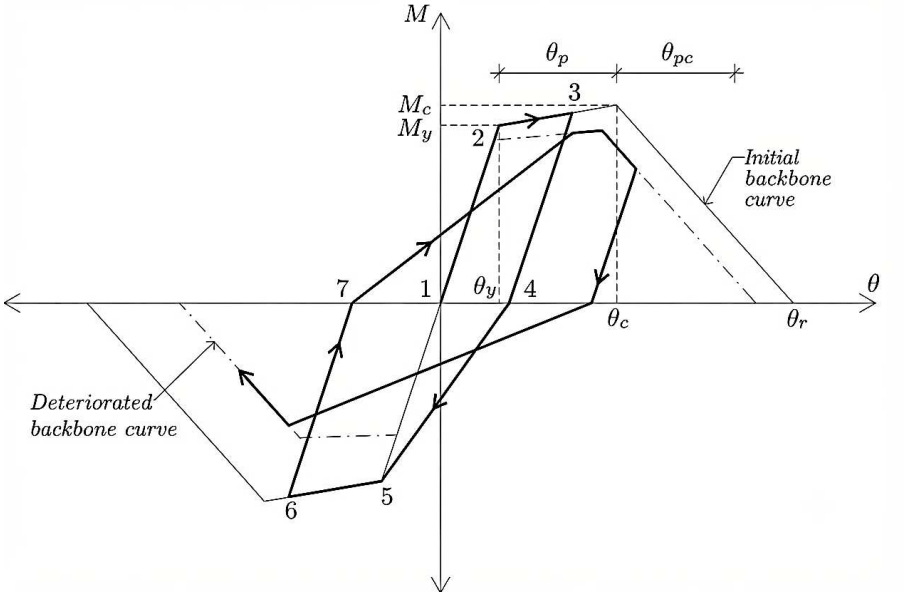



**Figure 5.** Schematic of the IMK model.

## 5. Discussion of the results

### *5.1. Incremental dynamic analysis*

Fig. 6 presents the results of the Incremental Dynamic Analysis (IDA) performed on three-dimensional (3D) building models. The IDA curves (in gray) are plotted with the Maximum Interstory Drift Ratio (MIDR) on the X-axis versus the 5%-damped spectral acceleration at the fundamental vibration period, $Sa(T_1, 5\%)$, for 1-, 2-, 4-, and 8-story buildings subjected to both unidirectional (UNI) and bidirectional (BID) seismic excitations. Also, the design spectral acceleration corresponds to the Maximum Considered Earthquake, $Sa_{MCE}$, and the Median Collapse Intensity, $Sa_{median}$, computed as the median of the collapse points identified on the IDA curves (black dot markers), can be observed. Following the FEMA P695 methodology (FEMA, 2009), the collapse capacity is quantified through the CMR, defined as $CMR = Sa_{median}/Sa_{MCE}$. Therefore, the CMR quantifies a structure's collapse capacity relative to its design seismic demand for the MCE. A consistent reduction in collapse capacity is observed when bidirectional ground motions are considered. Specifically, the CMR decreases by 6.6%, 18.1%, 30.1%, and 16.3% for the 1-, 2-, 4-, and 8-story buildings, respectively. This trend indicates that bidirectional seismic interaction increases inelastic demand, leading to an earlier onset of dynamic instability and collapse. Consequently, conventional UNI assessments may overestimate the collapse capacity of RC buildings.

The observed reduction in collapse capacity aligns with prior studies on BID seismic excitation. Gwalani et al. (2021) report that BID ground motions significantly increase the collapse probability and seismic fragility of RC frame buildings compared with conventional UNI analyses, primarily due to interactions between axial load fluctuations and biaxial

bending demands in columns. Similarly, Özcan and Binici (2022) demonstrated that biaxial loading substantially reduces the plastic rotation capacity of RC columns compared with uniaxial loading. More recently, Acharjya et al. (2024) emphasized that UNI analyses cannot capture important BID phenomena, including interaction effects, nonlinear load paths, and the associated stiffness and strength degradation mechanisms. Likewise, Li et al. (2024) showed that multidirectional ground motions significantly alter the distribution of seismic demands and damage in RC structures. These studies provide a consistent explanation for the reduction in collapse capacity observed in the present work, underscoring the importance of explicitly accounting for BID seismic excitation in collapse assessment.

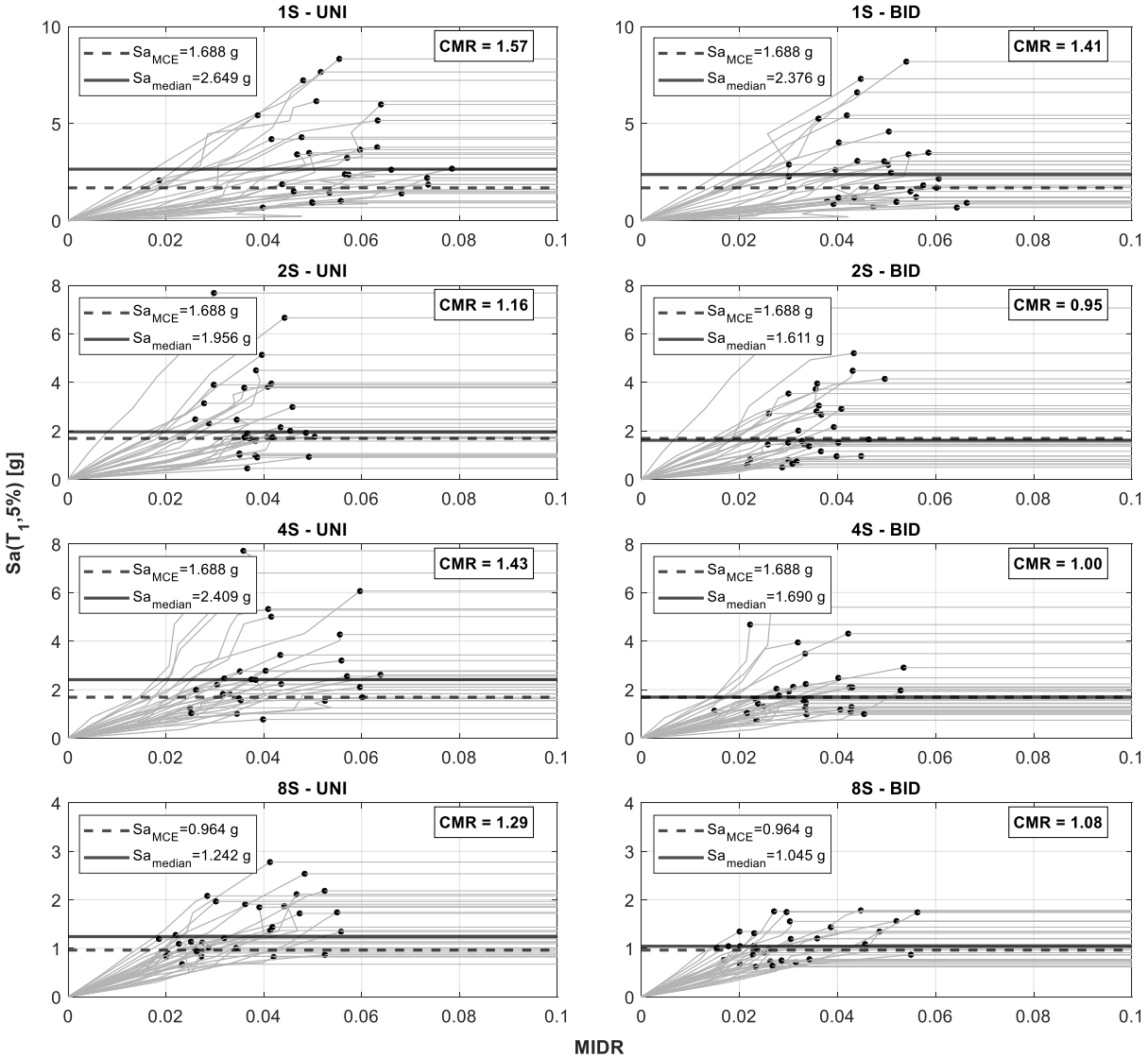



**Figure 6.** IDA results for UNI and BID analyses of the 3D buildings.

Fig. 7 presents the collapse fragility curves derived from the IDA collapse points (CP) shown in Fig. 6 for UNI and BID seismic excitations. The fragility functions provide a probabilistic representation of collapse using a lognormal distribution, characterized by the $Sa_{median}$ and the logarithmic standard deviation ($\beta$). It also provides the design spectral acceleration corresponding to the MCE ($Sa_{MCE}$), together with the median collapse intensities for the UNI and BID cases, shown as vertical lines. The corresponding values of $Sa_{median}$, $\beta$, and the CMR are summarized in Table 3. As

noted earlier, Fig. 7 and Table 3 consistently show that BID seismic excitation shifts the fragility curves toward lower spectral acceleration levels for all buildings, resulting in lower median collapse intensities and, consequently, lower CMR values.

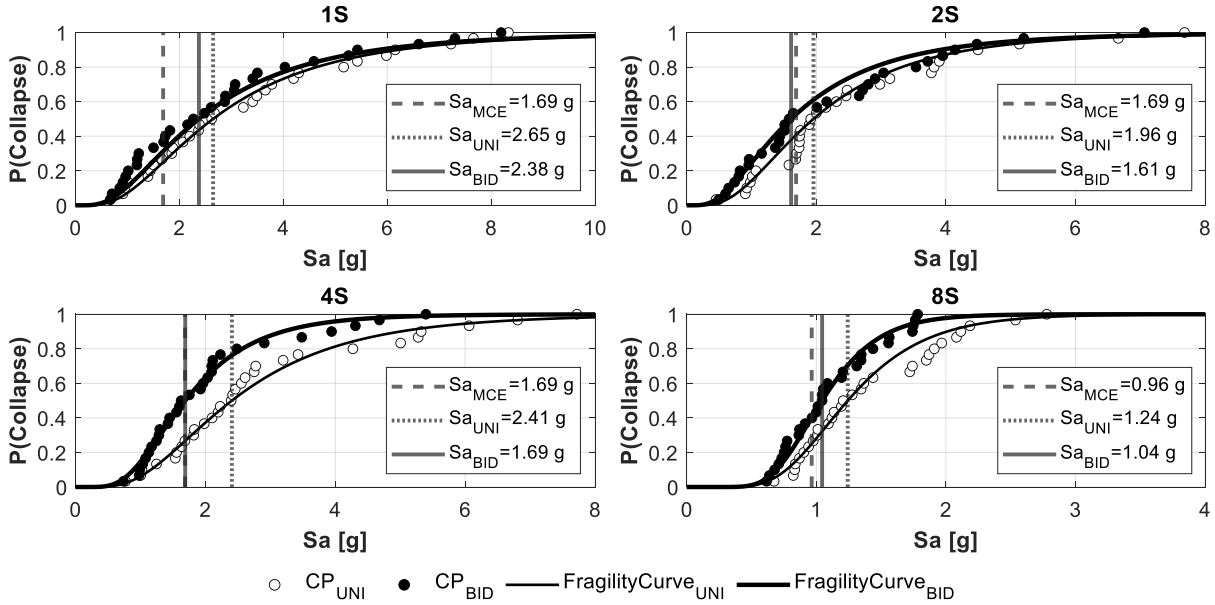



**Figure 7.** Comparison of collapse fragility curves for 1-, 2-, 4-, and 8-story RC buildings *subjected to* UNI and BID seismic excitations.

**Table 3**
Summary of collapse fragility parameters and CMRs for RC buildings subjected to UNI and BID seismic excitations.

| Building model | Seismic action | $Sa_{median}$ | $\beta$ | CMR |
|---|---|---|---|---|
| **1S** | UNI | 2.65 | 0.6658 | 1.57 |
| | BID | 2.38 | 0.7009 | 1.41 |
| **2S** | UNI | 1.96 | 0.6286 | 1.16 |
| | BID | 1.61 | 0.6937 | 0.95 |
| **4S** | UNI | 2.41 | 0.5700 | 1.43 |
| | BID | 1.69 | 0.4965 | 1.00 |
| **8S** | UNI | 1.24 | 0.3749 | 1.29 |
| | BID | 1.04 | 0.3215 | 1.08 |

The logarithmic standard deviation ($\beta$) characterizes the record-to-record variability of the collapse capacity and, therefore, the fragility function's dispersion. Larger values of $\beta$ indicate a wider distribution of collapse intensities and greater sensitivity of the structural response to the characteristics of individual ground motions, whereas smaller values correspond to a more concentrated distribution around the median collapse capacity, indicating a more consistent collapse response across seismic records. Compared with the UNI case, BID excitation increases $\beta$ by 5.3% and 10.4% for the 1- and 2-story buildings, respectively, indicating greater record-to-record variability in the collapse capacity of these low-rise structures. In contrast, for the 4- and 8-story buildings, BID excitation reduces $\beta$ by 12.9% and 14.2%, respectively, indicating that, despite reaching collapse at lower intensity levels, the collapse capacities are distributed over a narrower range of spectral accelerations. Notably, the low-rise buildings (1S, 2S, and 4S) exhibit the largest values of $\beta$ (0.6658–0.7009), whereas the 8-story building presents the lowest values (0.3215–0.3749), indicating that the collapse capacity

of taller buildings is less sensitive to the characteristics of individual ground motions. Overall, these results indicate that the primary effect of BID seismic excitation is a reduction in the median collapse capacity, whereas its influence on record-to-record variability depends on the building's structural characteristics.

### *5.2. Performance evaluation*

The structural collapse performance was evaluated using the Adjusted Collapse Margin Ratio (ACMR), which accounts for the effect of spectral shape on collapse capacity (FEMA, 2009). The ACMR is computed by multiplying the CMR by the Spectral Shape Factor (SSF), i.e., $ACMR = CMR \cdot SSF$. The resulting ACMR is then evaluated against acceptance criteria that depend on how the structural system's total uncertainty was modeled. For bidirectional ground motions, the computed ACMR values are further amplified by a factor of 1.2 to account for the additional seismic demand associated with multidirectional excitation (FEMA, 2009).

In this context, archetype models must be grouped into Performance Groups (PGs) based on similarities in their seismic response characteristics, primarily their fundamental vibration period. Each group should include at least three archetypes to ensure a statistically meaningful evaluation of collapse performance. In this study, the buildings were classified into two Performance Groups: PG1, representing short-period structures, and PG2, representing intermediate-period structures. Accordingly, the 1-, 2-, and a fictitious 3-story building were assigned to PG1, whereas the 4- and 8-story buildings were assigned to PG2. The fictitious 3-story archetype was introduced solely to meet the minimum requirement of three archetypes in PG1. Its CMR and ACMR values were estimated by linear interpolation between the corresponding results for the 2- and 4-story buildings. No additional fictitious archetype was incorporated into PG2, since introducing an intermediate-height building (e.g., a 6-story building) would not significantly affect the group-average ACMR or the corresponding acceptance outcome. Extending the analysis to a broader range of building heights would allow the inclusion of long-period structures and the definition of an additional Performance Group, which could be addressed in future studies to further investigate how structural vibration period influences the calibration of seismic response modification factors.

Table 4 summarizes the ACMR values for each building and PGs, together with the FEMA P695 acceptance criteria (Accept. ACMR) (FEMA, 2009). At the individual archetype level, all buildings satisfy the collapse performance requirements except the 2-story building, whose ACMR remains below the required threshold under both UNI and BID seismic excitations. At the Performance Group level, however, neither PG1 nor PG2 meets the required acceptance criterion, even though most individual archetypes meet the corresponding requirement. This difference arises because the individual and group evaluations are associated with collapse probabilities of 20% and 10%, respectively. PG1 attains average ACMR values of 1.67 and 1.66 under UNI and BID loading, corresponding to 93.8% and 93.3% of the required threshold (ACMR = 1.78), whereas PG2 reaches 1.75 and 1.61, equivalent to 98.3% and 90.4% of the required value. Notably, the unidirectional response of PG2 falls short of the acceptance criterion by only 1.7%, while the deficit increases to 9.6% under bidirectional excitation.

Although bidirectional excitation consistently reduces the CMR, this reduction is partially compensated in the FEMA P695 (FEMA, 2009) performance evaluation through the amplification factor of 1.2 applied to the ACMR. As a result, the differences between the UNI and BID ACMR values become significantly smaller than those observed for the corresponding CMR values. For the 1-story building, the amplified BID ACMR (2.13) is even higher than the unidirectional value (1.98). Similarly, the 2- and 8-story buildings exhibit nearly identical ACMR values under both loading conditions (1.40 vs. 1.39 and 1.65 vs. 1.66, respectively), indicating that the prescribed amplification factor effectively offsets the reduction in collapse capacity. In contrast, the 4-story building still shows a lower BID ACMR (1.56) than the unidirectional value (1.86), suggesting that, for this archetype, the reduction in collapse capacity exceeds the compensation provided by the 1.2 amplification factor.

**Table 4**
Collapse margin parameters and FEMA P695 acceptance results.

| PG No. | Building model | Collapse Margin Parameters | | | Acceptance Check | |
|---|---|---|---|---|---|---|
| | | CMR (UNI – BID) | SSF | ACMR (UNI – BID) | Accept. ACMR | Pass/Fail (UNI – BID) |
| PG1 | 1S | 1.57 - 1.41 | 1.26 | 1.98 - 2.13 | 1.46 | Pass - Pass |
| | 2S | 1.16 - 0.95 | 1.21 | 1.40 - 1.39 | 1.46 | Fail - Fail |
| | 3S | 1.29 - 0.98 | - | 1.63 - 1.47 | 1.46 | Pass - Pass |
| | **Mean of PG:** | **1.34 - 1.11** | **1.24** | **1.67 - 1.66** | **1.78** | **Fail - Fail** |
| PG2 | 4S | 1.43 - 1.00 | 1.30 | 1.86 - 1.56 | 1.46 | Pass - Pass |
| | 8S | 1.29 - 1.08 | 1.28 | 1.65 - 1.66 | 1.46 | Pass - Pass |
| | **Mean of PG:** | **1.36 - 1.04** | **1.29** | **1.75 - 1.61** | **1.78** | **Fail - Fail** |

*5.3. Calibration of the response modification factor*

Because the reference buildings designed with the code-prescribed response modification factor (R = 8) did not meet the PG acceptance criteria, an iterative calibration of R was performed. The complete collapse assessment procedure was then repeated for structural systems designed with R = 7, 6, 5, and 4 to identify the minimum value that satisfied the required ACMR acceptance criterion.

Fig. 8 presents the collapse fragility curves, and the IDA collapse points (unfilled markers) for the 1-, 2-, 4-, and 8-story buildings designed with different response modification factors under bidirectional seismic excitation, which is the focus of this study. The figure illustrates the progressive increase in collapse capacity as the response modification factor decreases. The corresponding fragility parameters, $Sa_{median}$ and $\beta$, are summarized in Table 5, providing a quantitative description of the collapse capacity and its record-to-record variability for each design case.

The collapse fragility parameters in Table 5 show that reducing the response modification factor R increases $Sa_{median}$ for all building heights, confirming that designs with lower R values have greater collapse capacity. This trend is expected because a decrease in R leads to higher design forces and, consequently, stronger structural systems that can withstand greater seismic intensities before collapse. However, the rate of improvement varies across the archetypes. The increase in $Sa_{median}$ is relatively modest for the 2-story building, rising from 1.61 g (R=8) to 2.14 g (R=4). By contrast, the 1-

and 4-story buildings exhibit more pronounced gains, with increases of approximately 61% (2.38 g to 3.82 g) and 50% (1.69 g to 2.53 g), respectively. The 8-story building also shows a significant increase in collapse capacity, with $Sa_{median}$ rising from 1.05 g (R = 8) to 1.31 g (R = 4), corresponding to an increase of approximately 25%. Although this increase is smaller than that observed for the 1- and 4-story buildings, it shows that reducing the response modification factor remains effective at enhancing collapse resistance, even for more flexible, long-period structures. These results indicate that the sensitivity of collapse capacity to the selected response modification factor depends on the structural characteristics of each archetype rather than following a uniform trend with building height.

The logarithmic standard deviation ($\beta$) behaves differently. For the 1- and 2-story buildings, $\beta$ remains nearly constant, varying only between approximately 0.69 and 0.74 despite the reduction in R. This suggests that lowering the response modification factor primarily shifts the median collapse capacity while producing little change in record-to-record variability. In contrast, the 4-story building shows a substantial increase in $\beta$, from 0.50 for R=8 to 0.70 for R=4, indicating a broader distribution of collapse intensities and, therefore, greater sensitivity of collapse capacity to ground-motion characteristics. The 8-story building shows a different response, with $\beta$ remaining consistently low, ranging from 0.25 to 0.35 across all R values, and no clear monotonic trend. These relatively small values indicate a narrow dispersion of collapse capacity, suggesting that the long-period structure's collapse response is less sensitive to record-to-record variability than that of the shorter-period archetypes. Consequently, although lower R values generally increase the median collapse capacity, they do not necessarily reduce the uncertainty associated with collapse, as the effect on record-to-record variability depends on the structural system considered.

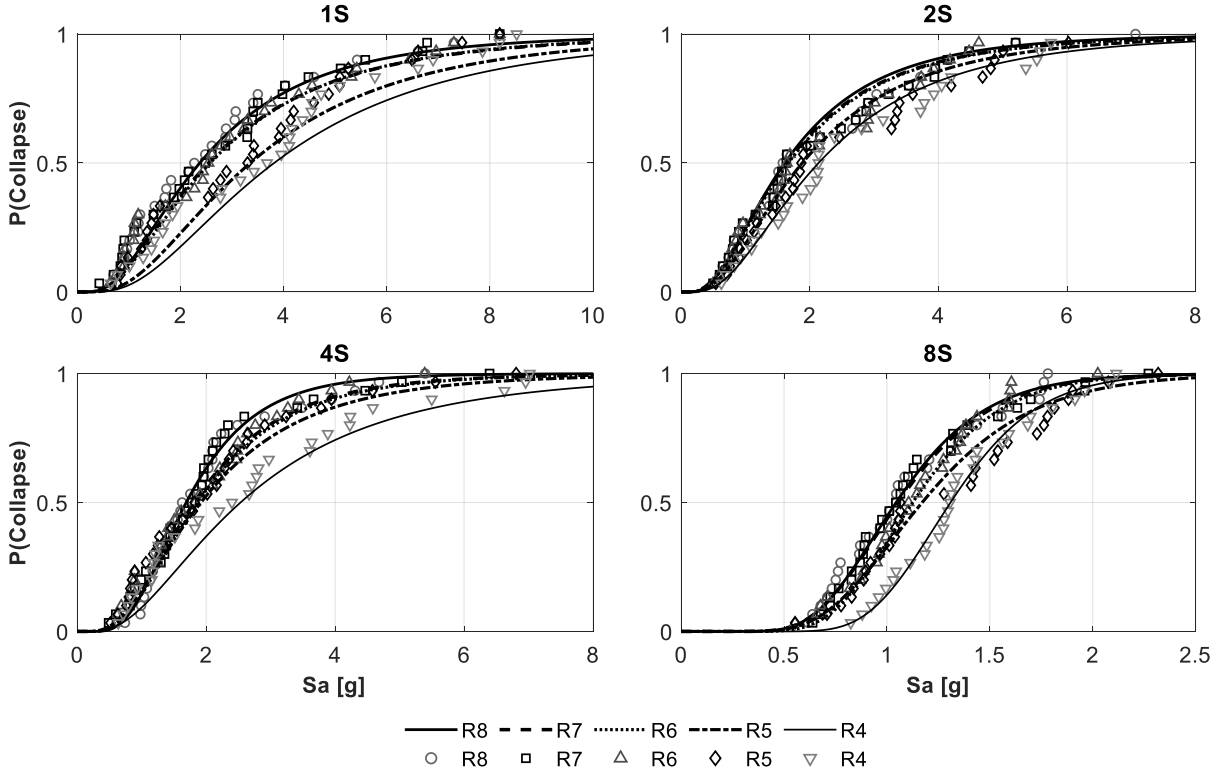



**Figure 8.** Effect of the response modification factor R on the collapse fragility of 1-, 2-, 4-, and 8-story RC buildings subjected to BID seismic excitation.

Table 6 summarizes the evolution of the ACMR for the analyzed buildings as the factor R is progressively reduced from 8 to 4 under bidirectional seismic excitation. As noted earlier, decreasing R consistently increases the ACMR across all archetypes, reflecting the higher design strength associated with lower response modification factors and the resulting improvement in collapse capacity.

**Table 5**
Effect of the response modification factor R on the collapse fragility parameters of RC buildings subjected to BID seismic excitation.

| Building model | Parameter | $R_8$ | $R_7$ | $R_6$ | $R_5$ | $R_4$ |
|---|---|---|---|---|---|---|
| **1S** | $Sa_{median}$ | 2.376 | 2.546 | 2.579 | 3.357 | 3.818 |
| | $\beta$ | 0.7009 | 0.7427 | 0.7287 | 0.6923 | 0.6925 |
| **2S** | $Sa_{median}$ | 1.611 | 1.639 | 1.667 | 1.884 | 2.137 |
| | $\beta$ | 0.6937 | 0.7228 | 0.7152 | 0.7112 | 0.6941 |
| **4S** | $Sa_{median}$ | 1.690 | 1.814 | 1.865 | 1.919 | 2.533 |
| | $\beta$ | 0.4965 | 0.5879 | 0.5857 | 0.6522 | 0.7027 |
| **8S** | $Sa_{median}$ | 1.045 | 1.054 | 1.125 | 1.171 | 1.309 |
| | $\beta$ | 0.3215 | 0.327 | 0.2973 | 0.3544 | 0.2512 |

For Performance Group 1 (PG1), the mean ACMR increases from 1.66 at R = 8 to 1.74, 1.76, 2.07, and 2.42 at R = 7, 6, 5, and R = 4, respectively. Considering the acceptance criterion (FEMA, 2009) for Performance Groups (ACMR = 1.78), the first response modification factor that satisfies the required collapse performance is R = 5. Likewise, for Performance Group 2 (PG2), the mean ACMR increases from 1.61 (R = 8) to 1.67, 1.72, 1.76, and 2.07 as R decreases. In this case, R = 5 remains marginally below the acceptance threshold (-3.37%), whereas R = 4 is the first value that satisfies the group-level criterion. These results demonstrate the systematic improvement in collapse performance achieved by lowering the response modification factor.

**Table 6**
Influence of the response modification factor R on the ACMR for the analyzed RC buildings.

| PG No. | Building model | ACMR | | | | |
|---|---|---|---|---|---|---|
| | | $R_8$ | $R_7$ | $R_6$ | $R_5$ | $R_4$ |
| PG1 | 1S | 2.13 | 2.28 | 2.31 | 2.96 | 3.34 |
| | 2S | **1.39** | **1.41** | **1.42** | 1.61 | 1.87 |
| | 3S | 1.47 | 1.54 | 1.55 | 1.66 | 2.04 |
| | **Mean of PG:** | **1.66** | **1.74** | **1.76** | 2.07 | 2.42 |
| PG2 | 4S | 1.56 | 1.68 | 1.68 | 1.71 | 2.22 |
| | 8S | 1.66 | 1.67 | 1.76 | 1.82 | 1.92 |
| | **Mean of PG:** | **1.61** | **1.67** | **1.72** | **1.76** | 2.07 |

A key aspect of the FEMA P695 evaluation is selecting an appropriate response modification factor for assessing PGs. In this regard, the calibrated values from the iterative collapse assessment are remarkably consistent with those predicted by the basic factor R formulation proposed by Garcia et al. (2024), which was developed using Peruvian and Chilean ground motions and explicitly accounts for bidirectional seismic effects. This formulation expresses the factor R as a function of the fundamental vibration period $T$ and the target displacement ductility ratio $\mu$. For comparison, fundamental vibration periods from modal analysis were paired with a target ductility ratio of $\mu = 8$. The resulting response

modification factors were R = 4.4, 4.9, 4.9, and 4.9 for the 1-, 2-, 4-, and 8-story buildings, respectively. These values are in close agreement with the previously calibrated range of R = 4 – 5. This agreement provides independent support for the applicability of the formulation proposed by Garcia et al. (2024), showing that it yields response modification factors consistent with the collapse performance objectives established by FEMA P695 (FEMA, 2009) for RC buildings subjected to bidirectional seismic excitation.

### *5.4. 2DOF results*

The use of detailed three-dimensional (3D) building models within the Incremental Dynamic Analysis (IDA) framework provides a rigorous representation of structural response; however, it entails a high computational cost. Even when implemented in a high-performance, non-graphical computing environment such as OpenSees, each nonlinear time-history analysis requires considerable processing time due to the structural model's complexity, the number of integration steps required for long-duration ground motions, and the iterative nature of the solution algorithms. As observed in this study, the IDA of a single ground-motion record required approximately 4 to 8 hours of computational time using about 12 intensity levels. When multiple ground motions and different values of R are considered, this computational demand becomes a major limitation for comprehensive parametric studies.

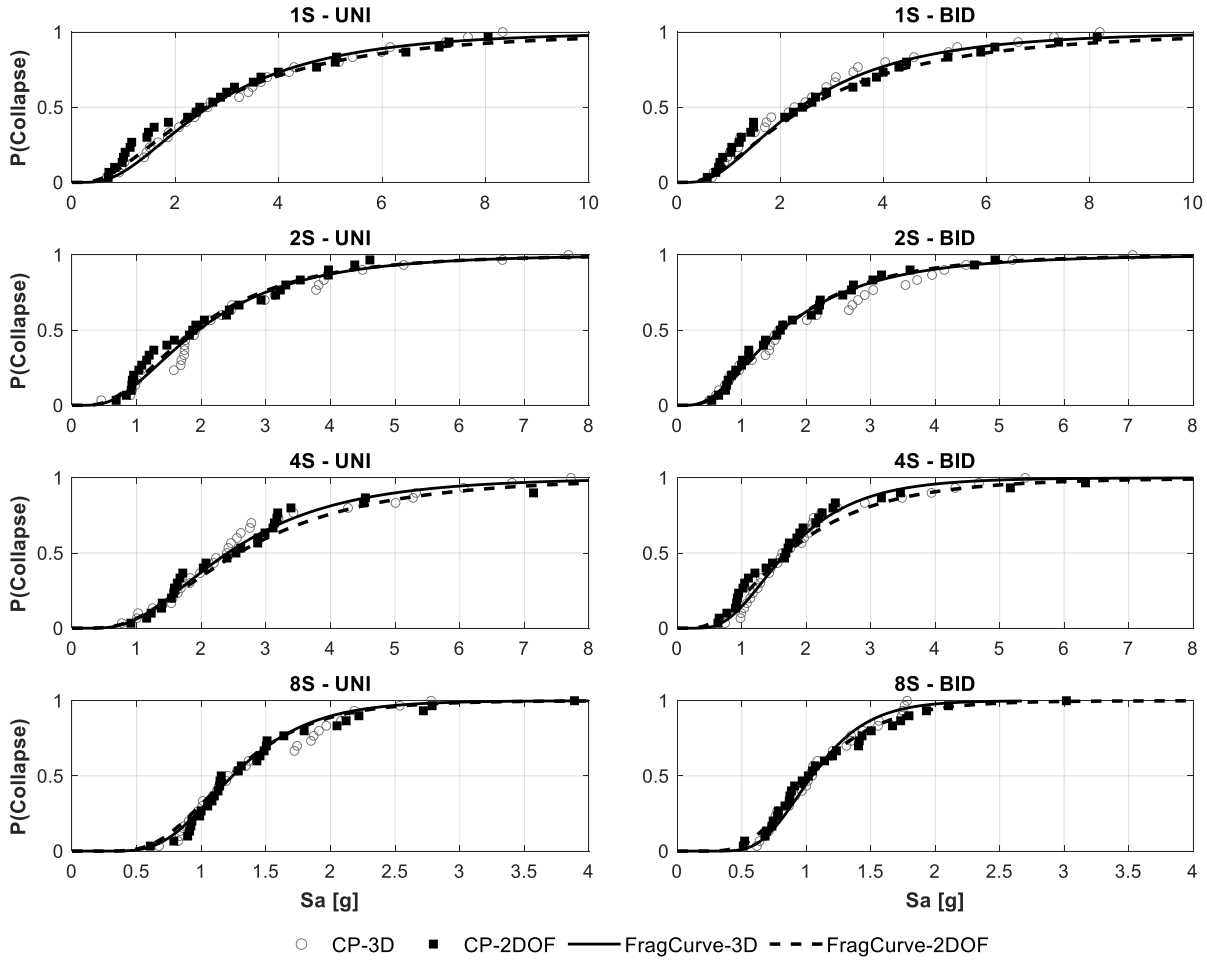



**Figure 9.** Comparison of collapse fragility curves for 1-, 2-, 4-, and 8-story RC buildings and their corresponding 2DOF models at R = 8.

To overcome this limitation, simplified single-degree-of-freedom (SDOF) and two-degree-of-freedom (2DOF) systems were used as computationally efficient alternatives to the 3D nonlinear models. The corresponding IDA analyses required only an average of 30 s per ground-motion record, making it feasible to evaluate a substantially larger number of intensity levels and obtain higher-resolution IDA curves while accurately reproducing the global seismic response under both UNI and BID excitations.

Fig. 9 presents fragility curves for 1-, 2-, 4-, and 8-story buildings designed with R = 8, comparing responses to UNI and BID seismic excitations for both the detailed 3D models and the corresponding SDOF and 2DOF idealizations. Overall, the results show strong agreement between simplified and detailed representations, with similar trends in the median spectral acceleration at collapse and in the dispersion of the fragility functions.

**Table 7**
Comparison of $Sa_{median}$ values between 3D nonlinear models and equivalent 2DOF systems under BID seismic excitation.

| Building | | Model | $R_8$ | $R_7$ | $R_6$ | $R_5$ | $R_4$ |
|---|---|---|---|---|---|---|---|
| **1S** | $Sa_{median}$ | 3D | 2.38 | 2.55 | 2.58 | 3.36 | 3.82 |
| | | 2DOF | 2.52 | 2.61 | 2.57 | 2.71 | 2.83 |
| | | error | 5.9% | 2.4% | -0.5% | -19.4% | -25.8% |
| | $\beta$ | 3D | 0.7009 | 0.7427 | 0.7287 | 0.6923 | 0.6925 |
| | | 2DOF | 0.7993 | 0.7919 | 0.7923 | 0.7815 | 0.7834 |
| | | error | 14.0% | 6.6% | 8.7% | 12.9% | 13.1% |
| **2S** | $Sa_{median}$ | 3D | 1.61 | 1.55 | 1.67 | 1.88 | 2.14 |
| | | 2DOF | 1.62 | 1.62 | 1.66 | 1.87 | 2.13 |
| | | error | 0.3% | 4.0% | -0.7% | -0.6% | -0.4% |
| | $\beta$ | 3D | 0.6937 | 0.7199 | 0.7152 | 0.7112 | 0.6941 |
| | | 2DOF | 0.6678 | 0.6718 | 0.6787 | 0.6888 | 0.6778 |
| | | error | -3.7% | -6.7% | -5.1% | -3.1% | -2.3% |
| **4S** | $Sa_{median}$ | 3D | 1.69 | 1.81 | 1.87 | 1.92 | 2.53 |
| | | 2DOF | 1.70 | 1.74 | 1.78 | 1.96 | 2.23 |
| | | error | 0.7% | -4.0% | -4.5% | 2.2% | -12.1% |
| | $\beta$ | 3D | 0.4965 | 0.5879 | 0.5857 | 0.6522 | 0.7027 |
| | | 2DOF | 0.6455 | 0.6377 | 0.6339 | 0.6246 | 0.6162 |
| | | error | 30.0% | 8.5% | 8.2% | -4.2% | -12.3% |
| **8S** | $Sa_{median}$ | 3D | 1.05 | 1.05 | 1.13 | 1.17 | 1.31 |
| | | 2DOF | 1.03 | 1.05 | 1.06 | 1.14 | 1.31 |
| | | error | -1.2% | -0.3% | -5.6% | -2.5% | 0.3% |
| | $\beta$ | 3D | 0.3215 | 0.327 | 0.2973 | 0.3544 | 0.2512 |
| | | 2DOF | 0.4129 | 0.4232 | 0.4141 | 0.3908 | 0.4215 |
| | | error | 28.4% | 29.4% | 39.3% | 10.3% | 67.8% |

This consistency is further quantified in Table 7, which summarizes $Sa_{median}$ and $\beta$ for the bidirectional analyses only, as these analyses constitute the primary objective of this study. For the 2-, 4-, and 8-story buildings, the equivalent 2DOF formulation accurately reproduced the median collapse capacity ($Sa_{median}$). Relative differences remained below 6% for the 2- and 8-story buildings across all R values, with most cases showing errors of less than 1%. The 4-story building showed discrepancies generally below 5%, except at R = 4, where the error increased to approximately 12%. In contrast,

the 1-story building exhibited larger discrepancies at R = 5 and R = 4, with the 2DOF model underestimating $Sa_{median}$ by 19.4% and 25.8%, respectively. Overall, the proposed formulation reproduced the collapse capacity of the 3D buildings in nearly all cases, with the largest discrepancies occurring only in the 1-story building designed with the lowest R values.

In contrast to $Sa_{median}$, the agreement in $\beta$ was more variable. The closest agreement was observed for the 2-story building, with relative differences ranging from −2.3% to −6.7%, whereas the 1-story building systematically overestimated $\beta$ by approximately 7% – 14%. Larger discrepancies were observed for the 4- and 8-story buildings, reaching approximately 30% and 68%, respectively, indicating that the simplified formulation reproduces the median collapse capacity more accurately than the collapse fragility functions' dispersion.

Within the FEMA P695 methodology, collapse performance is governed primarily by $Sa_{median}$ and the resulting ACMR values, whereas $\beta$ mainly characterizes the dispersion of the fragility function. Consequently, the close agreement achieved in $Sa_{median}$ and ACMR demonstrates that the proposed 2DOF formulation captures the dominant features of collapse performance while requiring only a fraction of the computational effort of detailed 3D nonlinear models. This enables efficient preliminary calibration of response modification factors and verification of ACMR acceptance criteria, reserving detailed 3D IDA analyses for final validation of the selected R values.

## 6. Conclusions

This study investigated how the response modification factor R affects the bidirectional seismic behavior and collapse capacity of 1-, 2-, 4-, and 8-story RC buildings using a combined approach of Incremental Dynamic Analysis (IDA) and the FEMA P695 methodology (FEMA, 2009). Detailed three-dimensional (3D) nonlinear models were subjected to unidirectional (UNI) and bidirectional (BID) ground motions in OpenSees. In parallel, equivalent two-degree-of-freedom (2DOF) systems incorporating an elliptical bidirectional yield surface and an IMK-based hysteretic model were developed as a computationally efficient alternative for collapse assessment. The study evaluated the influence of bidirectional seismic excitation on collapse performance, examined the ability of the proposed 2DOF models to reproduce the collapse behavior of the corresponding 3D buildings, and assessed the response modification factors required to satisfy the collapse performance criteria. The main findings of the study are summarized as follows:

1) BID seismic excitation reduced the CMR by 6.6%, 18.1%, 30.1%, and 16.3% for the 1-, 2-, 4-, and 8-story buildings, respectively, relative to UNI excitation.
2) Reducing R increased the median collapse capacity from 25% to 61%, indicating that the effectiveness of this design strategy depends on the building's structural configuration.
3) The 1-, 2-, and 4-story buildings consistently exhibited higher logarithmic standard deviations (β = 0.4965 – 0.7427) than the 8-story building (β = 0.2512 – 0.3544), indicating that the 8-story building's collapse capacity was considerably less sensitive to record-to-record variability.

4) Using the design value of R = 8, neither PG met the FEMA P695 acceptance criterion, achieving only 93.3% and 90.4% of the required ACMR for PG1 and PG2, respectively. Compliance required R values of 4 to 5, depending on the structural system.
5) The proposed 2DOF methodology reproduced the median collapse capacity of the 3D buildings, with relative errors below 6% in nearly all cases, enabling efficient preliminary calibration of the response modification factor R.

**CRediT authorship contribution statement**

**Marco F. Garcia:** Methodology, Software, Formal analysis, Visualization, Writing – original draft. **Renzo J. Mejia:** Supervision, Software, Review, and Editing. **Victor I. Fernandez-Davila:** Conceptualization, Methodology, Supervision, Analysis, Writing – original draft, Review and Editing.

**Declaration of competing interests**

The author(s) declare that they have no known competing financial interests or personal relationships that could have appeared to influence the work reported in this paper.

**Data availability**

The ground-motion time series utilized in this publication were sourced from the National Hazards Risk and Resiliency Research Center (NHR3) website. The NHR3 data can be found on the following webpage: https://www.risksciences.ucla.edu/nhr3/nga-subduction/gmportal. The website source was accessed in April 2025.

**Acknowledgements**

This work presents original research independently conducted by the authors. The authors would like to thank the Faculty of Civil Engineering at Continental University and the Postgraduate Section in Civil Engineering at the Pontifical Catholic University of Peru for their support.

**Funding**

None.

**References**

ASCE/SEI 7-16. Minimum design loads for buildings and other structures. 2016.

ASCE/SEI 41-23. Seismic evaluation and retrofit of existing buildings. 2023.

Asociación Chilena de Sismología e Ingeniería Antisísmica. (2017) *Diseño sísmico basado en desempeño: Un procedimiento alternativo para el análisis y diseño sísmico de edificios*. Subcomité n.° 7 (In Spanish). https://www.achisina.cl/manuales-y-guias/

Chopra AK, Goel RK (2002) A modal pushover analysis procedure for estimating seismic demands for buildings. *Earthq Eng Struct Dyn*, *31*(3), 561-582. https://doi.org/10.1002/eqe.144

Chopra AK, Goel RK, Chintanapakdee C (2004) Evaluation of a modified MPA procedure assuming higher modes as elastic to estimate seismic demands. *Earthq Spectra*, *20*(3), 757-778. https://doi.org/10.1193/1.1775237

Chopra AK (2020) *Dynamics of structures: Theory and applications to earthquake engineering* (5th ed., SI units). Pearson Education Limited.

De Stefano M, Faella G (1996) An evaluation of the inelastic response of systems under biaxial seismic excitations. *Eng Struct*, *18*(9), 724-731. https://doi.org/10.1016/0141-0296(95)00216-2

Duruflé M, Grob P, Joly P (2009) Influence of Gauss and Gauss-Lobatto quadrature rules on the accuracy of a quadrilateral finite element method in the time domain. *Numerical Methods for Partial Differential Equations: An International Journal*, *25*(3), 526-551. https://doi.org/10.1002/num.20353

FEMA (2009) Quantification of Building Seismic Performance Factors. FEMA P695. Prepared by the Applied Technology Council for the Federal Emergency Management Agency, Washington, D.C. https://nehrpsearch.nist.gov/static/files/FEMA/fema_p695.pdf

Fernandez-Davila VI, Cominetti S, Cruz EF (2000) Considering the bi-directional effects and the seismic angle variations in building design. In *Proceedings 12th World Conf. on Earthq Eng.* Auckland, New Zealand.

Fernandez-Davila VI, Cruz EF (2008) *Estimating inelastic bi-directional seismic response of multi-story asymmetric buildings using a set of combination rules.* In *Proceedings 14th World Conf. on Earthq Eng.* China, Beijing.

Filippou FC, Popov EP, Bertero VV (1983) *Effects of bond deterioration on hysteretic behavior of reinforced concrete joints* (Report No. UCB/EERC-83/19). Earthquake Engineering Research Center, University of California, Berkeley. https://nehrpsearch.nist.gov/static/files/NSF/PB84192020.pdf

Garcia MF, Bazan JL, Fernandez-Davila VI (2024) Parametric evaluation of the response modification factor R considering bidirectional ground motions. *Soil Dyn Earthq Eng*, *186*, 108948. https://doi.org/10.1016/j.soildyn.2024.108948

Goel RK, Chopra AK (2005) Extension of modal pushover analysis to compute member forces. *Earthq Spectra*, *21*(1), 125-139. https://doi.org/10.1193/1.1851545

Gwalani P, Singh Y, Varum H (2022) Effect of bidirectional excitation on seismic performance of regular RC frame buildings designed for modern codes. *Earthq Spectra*, *38*(2), 950-980. https://doi.org/10.1177/87552930211047879

Haselton CB, Liel AB, Taylor-Lange SC, Deierlein GG (2016) Calibration of model to simulate response of reinforced concrete beam-columns to collapse. *ACI Struct Journal*, *113*(6), 1141-1152. https://doi.org/10.14359/51689245

Hussain MA, Dutta SC, Das S (2022a) Effect of bidirectional ground shaking on structures in the elastic and post-elastic range: Adequacy of design provisions. *Journal of Building Eng*, *45*, 103656.

Hussain MA, Dutta SC, Das S (2022b) Seismic behaviour of structures under bidirectional ground motion: Does the angle of incidence have any influence? *Soil Dyn Earthq Eng*, *159*, 107328. https://doi.org/10.1016/j.soildyn.2022.107328

Ibarra LF, Medina RA, Krawinkler H (2005) Hysteretic models that incorporate strength and stiffness deterioration. *Earthq Eng Struct Dyn*, *34*(12), 1489-1511. https://doi.org/10.1002/eqe.495

Kalman Šipoš T, Brandis A, Bohinc U, Ristić U (2025) Determining critical ground motion parameters for damage prediction in reinforced concrete frame existing buildings. *Applied Sciences*, *15*(5), 2326. https://doi.org/10.3390/app15052326

Kashani M, Salami MR, Goda K, Alexander N (2017) *Nonlinear flexural behaviour of RC columns including bar buckling and fatigue degradation*. *Magazine of Concrete Research, 70*(5), 231–247. https://doi.org/10.1680/jmacr.16.00495

Kwong NS, Chopra AK (2018) Determining bidirectional ground motions for nonlinear response history analysis of buildings at far-field sites. *Earthq Spectra*, *34*(4), 1931-1954. https://doi.org/10.1193/052217EQS093M

Mazzoni S (2022) *NGA-Subduction Portal: Ground-Motion Record Selection and Download* (Interactive resource). The B. John Garrick Institute for the Risk Sciences. https://www.risksciences.ucla.edu/nhr3/nga-subduction/gmportal

Mazzoni S, Scott MH (2024) *Efficient concentrated-plasticity modeling in OpenSees*. 18th World Conf. on Earthq Eng (WCEE2024), Milan, Italy.

McKenna F (1997) *Object-oriented finite element programming: Frameworks for analysis, algorithms and parallel computing* (Doctoral dissertation). University of California, Berkeley, CA, USA.

Menegotto M, Pinto PE (1973) *Method of analysis for cyclically loaded R.C. plane frames including changes in geometry and non-elastic behavior of elements under combined normal force and bending*. IABSE Reports of the Working Commissions, 13. http://doi.org/10.5169/seals-13741

Ministerio de Vivienda, Construcción y Saneamiento. Norma Técnica Peruana de Edificación E.060 Concreto Armado. 2009. El Peruano.

Ministerio de Vivienda, Construcción y Saneamiento. Norma Técnica Peruana de Edificación E.030 Diseño Sismorresistente. 2026. El Peruano.

Miranda E, Bertero VV (1994) Evaluation of strength reduction factors for earthquake-resistant design. *Earthq spectra*, *10*(2), 357-379. https://doi.org/10.1193/1.1585778

NIST (2010) "Evaluation of the FEMA P-695 methodology for quantification of building seismic performance factors." Gaithersburg, MD. https://www.nehrp.gov/pdf/nistgcr10-917-8.pdf

Özcan O, Binici B (2023) Plastic rotation capacity of RC columns under biaxial seismic demands. *Bull Earthq Eng*, *21*(4), 1979-2012. https://doi.org/10.1007/s10518-022-01597-4

Reyes JC, Kalkan E (2015a) Significance of rotating ground motions on behavior of symmetric-and asymmetric-plan structures: Part I. Single-story structures. *Earthq Spectra*, *31*(3), 1591-1612. https://doi.org/10.1193/072012EQS241M

Reyes JC, Kalkan E (2015b) Significance of rotating ground motions on behavior of symmetric-and asymmetric-plan structures: Part II. Multi-story structures. *Earthq Spectra*, *31*(3), 1613-1628. https://doi.org/10.1193/072012EQS242M

Roy A, Santra A, Roy R (2018) Estimating seismic response under bi-directional shaking per uni-directional analysis: Identification of preferred angle of incidence. *Soil Dyn Earthq Eng*, *106*, 163-181. https://doi.org/10.1016/j.soildyn.2017.12.022

Sarma SK, Yang KS (1987) An evaluation of strong motion records and a new parameter A95. *Earthq Eng Struct Dyn*, *15*(1), 119-132. https://doi.org/10.1002/eqe.4290150109

Scott BD, Park R, Priestley MJ (1982) *Stress-strain behavior of concrete confined by overlapping hoops at low and high strain rates*. *ACI Journal Proceedings, 79*(1), 13–27. https://doi.org/10.14359/10875

Stewart JP, Abrahamson NA, Atkinson GM, Baker JW, Boore DM, Bozorgnia Y, ... Sabol TA (2011) Representation of bidirectional ground motions for design spectra in building codes. *Earthq Spectra*, *27*(3), 927-937. https://doi.org/10.1193/1.3608001

Surana M, Singh Y, Lang DH (2018) Fragility analysis of hillside buildings designed for modern seismic design codes. *The Structural Design of Tall and Special Buildings*, *27*(14), e1500. https://doi.org/10.1002/tal.1500

Taucer F, Spacone E, Filippou FC (1991) A fiber beam-column element for seismic response analysis of reinforced concrete structures (Vol. 91). Berkeley, CA, USA: Earthquake Engineering Research Center, College of Engineering, University of California.

The MathWorks Inc. (2026) MATLAB version: 9.12.0.1884302 (R2026a), academic license: 40852604, Natick, Massachusetts. Available at: https://www.mathworks.com.

Vamvatsikos D, Cornell CA (2002a) *Incremental dynamic analysis. Earthq Eng Struct Dyn, 31(3)*, 491–514. https://doi.org/10.1002/eqe.141

Vamvatsikos D, Cornell CA (2002b) The incremental dynamic analysis and its application to performance-based earthquake engineering. In *Proceedings of the 12th European Conf. on Earthq Eng* (Vol. 40, pp. 1375-1392). 9 - 13 September 2002, Barbican Center, London, UK.

Wang F, Li HN, Zhang CQ, Zhang YZ (2023) Damage-based strength reduction factor spectra of structures subjected to bidirectional ground motions. *Advances in Struct Eng*, *26*(1), 72-88. https://doi.org/10.1177/13694332221119866